ACI STRUCTURAL JOURNAL TECHNICAL PAPER

Title no. 98-S77

Seismic Response of Multiple-Anchor Connections to Concrete

by Yong-Gang Zhang, Richard E. Klingner, and Herman L. Graves, III

The behavior under seismic loading of multiple-anchor connections to concrete was the ultimate objective of the research program discussed here. That research program addressed the static and dynamic behavior, under tension and shear (separately and in combination) of single and multiple-anchor connections to concrete. Effects of cracking and dynamic loading rates were addressed. This paper deals with the seismic response of multiple-anchor connections to concrete. Its most important conclusion is that multiple-anchor connections designed for ductile behavior in uncracked concrete under static loading will probably still behave in a ductile manner in cracked concrete under dynamic loading.

Keywords: anchors; connections; fasteners; seismic

OBJECTIVES AND SCOPE

The U.S. Nuclear Regulatory Commission (NRC) recently completed a research project they sponsored whose objective was to gather technical data on how the seismic behavior and strength of anchors (cast-in-place, expansion, and undercut) and their supporting concrete differ from the static behavior. To that end, a research program was carried out on the dynamic behavior of anchors in concrete. The research program comprised four tasks:

1. Static and dynamic behavior of single tensile anchors (250 tests);
2. Static and dynamic behavior of multiple tensile anchors (179 tests);
3. Static and dynamic behavior of near-edge anchors (150 tests); and
4. Static and dynamic behavior of multiple-anchor connections (16 tests).

The anchors tested were selected based on their reported frequency of use in nuclear power plants in the U.S. Anchors included cast-in-place headed bolts, grouted headed bolts, two wedge-type expansion anchors, one sleeve-type expansion anchor, and two undercut anchors. Loading conditions included tension, shear, and combined tension and shear. Test variables included different concrete strengths and types, loading rate, and the presence of cracks. In this paper, the seismic behavior of multiple-anchor connections (Task 4) is described. Results are discussed in more detail in Zhang (1997) and Klingner et al. (1998).

BACKGROUND

The behavior of anchors to concrete is discussed at length in CEB (1991) and in Klingner et al. (1998). Due to limitations of space, that material is not repeated here. Most tests on connections have been conducted to determine ultimate capacities under quasi-static, monotonic loading. A few studies have investigated the effects on connections of different types of loading, such as impact loading, seismic loading and reversed loading (Cannon 1981; Malik, Mendonca, and Klingner 1982; Copley and Burdette 1985; Collins, Klingner, and Polyzois 1989). In most of those tests, the loading patterns involved a particular dynamic loading pattern at a magnitude much smaller than the anchor's ultimate capacity, followed by a monotonic load to failure to investigate the effects of dynamic loading on ultimate load-displacement behavior (Copley and Burdette 1985; Collins, Klingner, and Polyzois 1989). Few data were available on the dynamic behavior of anchors with small embedment. Only a few investigations (Eibl and Keintzel 1989) existed regarding the influence of loading rate on the entire load-displacement behavior of anchors, including earlier tests in this project by Rodriguez (1995) and Lotze (1997). In addition, most connections had been tested in uncracked concrete. Some tests had been conducted in cracked concrete or in high-moment regions (Cannon 1981; Copley and Burdette 1985; Eibl and Keintzel 1989; and Eligehausen and Balogh 1995). Some of those tests, however, focused only on load-displacement behavior of anchors under service or factored loads (Cannon 1981; Copley and Burdette 1985). To the best of the authors' knowledge, the testing program described here represents the first published results of tests on multiple-anchor connections under seismic loading.

The tests of this project were conducted on post-installed anchors. Because anchor behavior as governed by tensile yield and fracture of the anchor shank is well-understood, the anchors were embedded at relatively shallow depths, and failed by concrete breakout, which can be reliably predicted by the CC Method (Fuchs, Eligehausen, and Breen 1995). For some post-installed anchors, that breakout was combined with pullout of the anchor from the hole, or by pull-through of the anchor with respect to the expansion mechanism. Such cases are noted in the following discussion.

TEST SETUP AND PROCEDURE

Anchors tested

Based on surveys of existing anchors in nuclear applications, the NRC was primarily interested in documenting the behavior of selected wedge-type expansion anchors, of selected undercut anchors, and also of anchors in cementitious grout. The testing program originally emphasized one wedge-type expansion anchor (referred to here as Expansion Anchor), with some tests on one undercut anchor (UC Anchor 1 [UC1]), and other tests on anchors in one type of cementitious grout (Grouted Anchor). As the testing progressed, other anchors were added: a variant on the expansion anchor (Expansion Anchor II [EAII]); another

ACI Structural Journal, V. 98, No. 6, November-December 2001.
MS No. 00-179 received August 17, 2000, and reviewed under Institute publication policies. Pertinent discussion will be published in the September-October 2002 *ACI Structural Journal* if received by May 1, 2002.

Yong-Gang Zhang *is an engineer at Han-Padron Associates, Houston, Tex.*

Richard E. Klingner, *FACI, is the Phil M. Ferguson Professor in Civil Engineering at the University of Texas at Austin. He is a former chair of ACI Committee 531, Masonry Structures Research, and Joint ACI-ASCE Committee 442, Response of Concrete Buildings to Lateral Forces. He is a member of ACI Committees 349, Concrete Nuclear Structures; 355, Anchorage to Concrete; 374, Performance-Based Seismic Design of Concrete Buildings; 523, Cellular Concrete; and Joint ACI-ASCE-TMS Committee 530, Masonry Standards. He is also a former member of ACI's Technical Activities Committee (TAC), and a current member of ACI's Educational Activities Committee (EAC). His research interests include dynamic response of masonry and concrete structures, and anchorage to concrete.*

ACI member **Herman L. Graves, III** *is a senior structural engineer at the U.S. Nuclear Regulatory Commission, Washington, D.C. He is a member of ACI Committee 349, Concrete Nuclear Structures, and 355, Anchorage to Concrete. His research interests include structural aging, soil-structure interaction, and anchorage to concrete.*

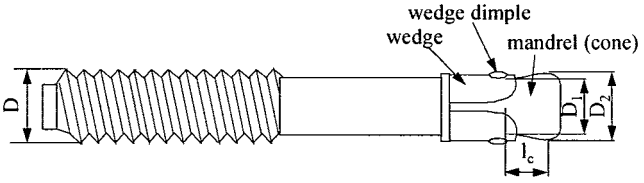

Fig. 1—Key dimensions of EAII.

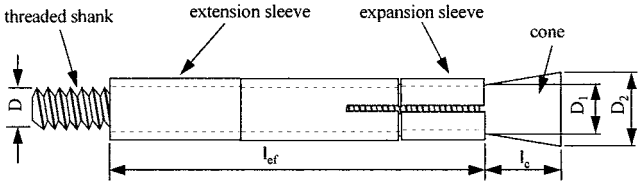

Fig. 2—Key dimensions of UC1.

undercut anchor (UC Anchor 2 [UC2]); and a heavy-duty sleeve-type single-cone expansion anchor (Sleeve Anchor). Based on current use in nuclear applications, it was decided to test anchors ranging in diameter from 3/8 to 1 in. (9.2 to 25.4 mm), with emphasis on 3/4 in. (19.1 mm) diameter. Tests in Task 4, described here, were conducted using EAII and UC1.

EAII—The EAII tested in this study is shown in Fig. 1. It is a wedge-type expansion anchor, installed in a pre-drilled hole slightly larger than the anchor diameter. The nut is torqued, raising the mandrel and expanding the wedge. Key dimensions of EAII are shown in Table 1. Samples of EAII were obtained from normal production of the manufacturer.

UC1—The UC1 tested throughout this study is a conventionally opening undercut anchor, consisting of a threaded rod with a steel cone at one end and an expansion sleeve. Key dimensions of UC1 are shown in Fig. 2 and Table 2. Using a universal testing machine, three tension tests in Task 2 of this program on three anchor shafts of UC1 of 5/8 in. (16 mm) diameter were performed (Lotze and Klingner 1997). The average ultimate strength was 912 N/mm^2 (132 kips/in.^{2}). The actual bearing area of UC1 anchors (the surface area of the undercut portion of the sleeve) is 3.25 in.^{2} (2097 mm^2) for 3/4 in. (19 mm) diameter anchors, 1.79 in.^{2} (1153 mm^2) for 5/8 in. (16 mm) diameter anchors, and 1.23 in.^{2} (794 mm^2) for 3/8 in. (10 mm) diameter anchors.

Embedment depths

For nuclear applications, the overall anchor design objective is to have failure governed by yield and fracture of anchor steel. The dynamic behavior of the anchor steel itself is relatively well-understood. The embedment depth selected for each task of this study depended on the failure mode under study. In Task 1, 2, and 3, to determine the influence of dynamic loading on anchor capacity as governed by concrete breakout, pullout or pull-through, shallow embedments were used, corresponding either to the manufacturer's standard embedment, or to the manufacturer's minimum recommended embedment. In Task 4, by contrast, anchors were embedded sufficiently to induce failure by yield and fracture of the anchor steel. The embedment depth was 7 in. (178 mm), calculated based on ACI 349 Appendix B (1990).

Table 1—Key dimensions of EAII

Anchor diameter D		D1		D2		l_c	
in.	mm	in.	mm	in.	mm	in.	mm
3/4	19.1	0.565	14.4	3/4	19.1	0.70	17.8

Table 2—Key dimensions of UC1

Anchor diameter D		Sleeve diameter		l_{ef}		D1		D2		l_c	
in.	mm	in.	mm	in.	mm	in.	mm	in.	mm	in.	mm
3/8	10.0	0.625	15.9	2.25	57.2	0.440	11.2	0.625	15.9	0.600	15.2
5/8	16.0	0.910	23.1	7.00	178.0	0.720	18.3	0.940	23.9	0.800	20.3
3/4	19.0	1.105	28.1	4.00	102.0	0.815	20.7	1.140	29.0	0.915	23.2

Table 3—Concrete mixture proportions

	Concrete mixture proportions				
Concrete	Cement, lb/yd^3	Coarse aggregate, lb/yd^3	Fine aggregate, lb/yd^3	Water, lb/yd^3	Retarder, oz/yd^3
4700 lb/in.^{2} river gravel	390	1876	1432	250	48

Concrete

The target concrete compressive strength for this testing program was 4700 lb/in.^{2} (32.4 MPa), with a permissible tolerance of ±500 lb/in.^{2} (±3.45 MPa) at the time of testing. This target value was selected because it is representative of concrete strengths in existing nuclear power plants. Mixture designs are shown in Table 3. One type of aggregate, a local river gravel, was used for the tests described here. The mixture had a slump of 4 in. (101 mm).

Test specimens were cast using ready-mix concrete, consolidated with mechanical vibrators, screeded, troweled, and covered with polyethylene sheets. Eighteen 6 in. (152 mm) diameter by 12 in. (305 mm) cylinders were usually cast with the test specimens and cured in laboratory air. The specimens were not tested until at least 28 days after casting, and until the desired strength had been reached.

Test setup

The overall test setup for Task 4 is shown in Fig. 3. Reversed cyclic loads were applied to the connection through a loading attachment, shown in Fig. 4. The stiff baseplate was 2 in. (51 mm) thick; the flexible one, 1 in. (25 mm). Both baseplates had stiffeners.

The external load on the connections was measured with a load cell. The tension in each anchor was measured with a force washer placed between the normal washer and the baseplate.

Displacements of the attachment include slip and rotation of the baseplate. The slip of the baseplate δ_{h1} in Fig. 5 was

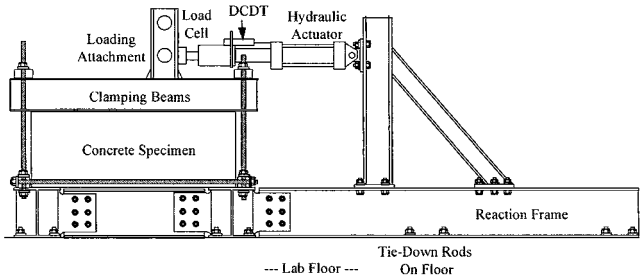

Fig. 3—Test setup for multiple-anchor tests of Task 4.

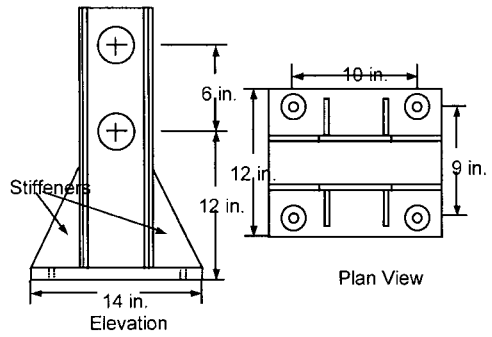

Fig. 4—Loading attachment used for Task 4.

measured with a potentiometer placed against the back of the baseplate. The displacement of the vertical beam at 12 in. (305 mm) from the surface δ_{h2} was also measured (Fig. 5). The rotation was calculated as the difference between these two horizontal displacements, assuming the beam to be infinitely stiff. The vertical displacement of the baseplate δ_v was measured at the centerline of the baseplate as well. It may not be a precise indicator of the rotation of the baseplate, however, due to the uneven concrete surface and the flexibility of the baseplate.

The rotation of the attachment can be calculated from Eq. (1)

$$\theta = \arctan\left(\frac{\delta_{h2} - \delta_{h1}}{12}\right) \quad (1)$$

where

θ = rotation of attachment;

δ_{h1} = transverse displacements measured at the baseplate; and

δ_{h2} = transverse displacements measured at 12 in. (305 mm) above concrete surface.

Seismic dynamic loading for Task 4

To simulate earthquake loading on the multiple-anchor attachments of Task 4 of this study, the displacement response of a typical attachment was estimated as follows:

The attachment was assumed to be a single-degree-of-freedom (SDOF) system with a concentrated mass at 12 in. (305 mm) above the concrete surface. Using the BDA5 program (discussed later in this paper) and the load-displacement curves from Task 2 of this research program (Lotze and Klingner 1997), the horizontal displacement and the rotation of the baseplate were estimated as functions of load (Fig. 6). This load-displacement curve was then simplified as bilinear (Fig. 6). The displacement at 12 in. (305 mm) from the concrete surface was calculated using the horizontal displacement and the baseplate rotation of the attachment. The yield load is 28 kips (125 kN), at a total displacement of 0.074 in.

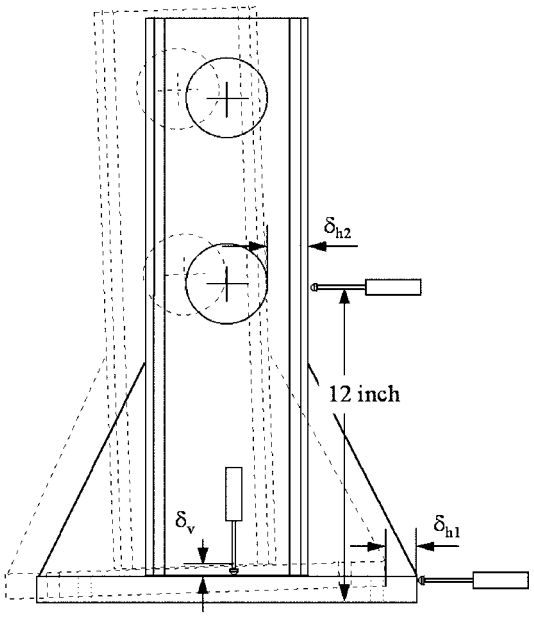

Fig. 5—Displacement instrumentation for multiple-anchor connection tests.

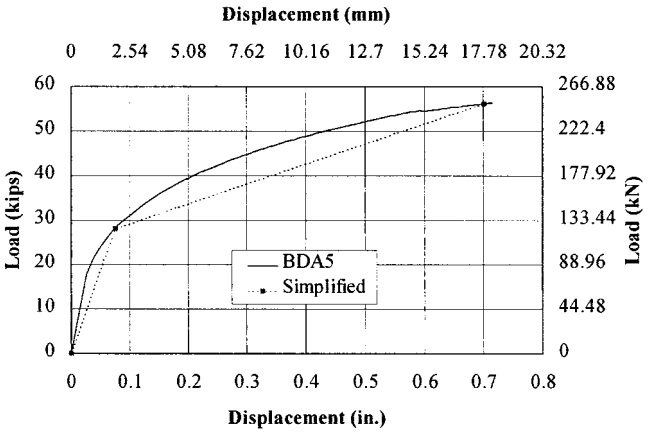

Fig. 6—Load-displacement curves from BDA5 and simplified for attachment.

(1.9 mm). The deformation of the beam at the maximum static capacity of 56 kips (249 kN), calculated using the BDA5 program, was 0.7 in. (17.8 mm).

The displacement ductility factor μ used to reduce the maximum calculated elastic acceleration was estimated as shown in Fig. 7 and calculated as follows

$$\mu = 0.70/\delta_{ela} = 0.70/(2 \times 0.074) = 4.73$$

Assuming the maximum earthquake ground acceleration as 0.4*g* and equivalent viscous damping of 5%, and considering displacement ductility, the maximum total response acceleration of the attachment is approximated as

$$\ddot{u}_{max} = \frac{0.4g \times 2.6}{\sqrt{2\mu - 1}} = \frac{0.4g \times 2.6}{\sqrt{2 \times 4.73 - 1}} = \quad (2)$$

$$0.36g \approx 0.4g = \ddot{u}_{max}$$

The corresponding equipment mass was estimated according to the yield strength of the attachment (the smaller of the

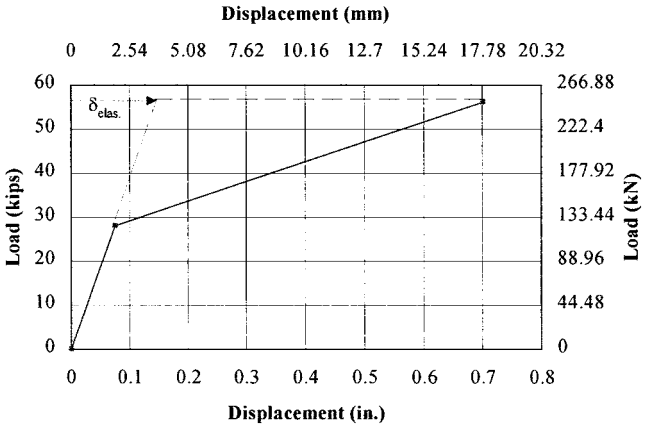

Fig. 7—Calculation of displacement ductility factor.

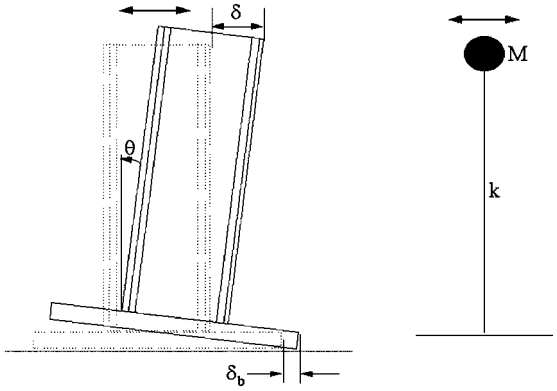

Fig. 8—Idealization of multiple-anchor attachment.

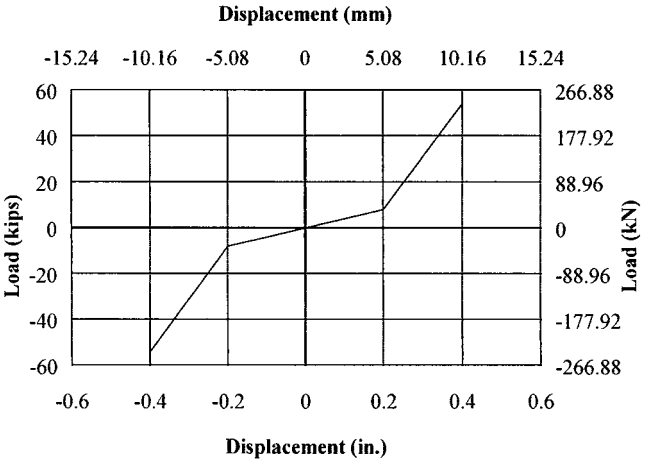

Fig. 9—Idealized load-displacement curves for multiple-anchor attachments.

flexural capacity of the attachment and the capacity of the anchor group) as

$$250 \text{ kN}/0.4g = 637{,}100 \text{ kg } (140 \text{ k-sec}^2/\text{in.}) \quad (3)$$

The previously mentioned parameters were used for initial estimates of attached mass and connection response. They were revised during testing. In a trial test, significant displacement occurred without much load, due to the gaps between the baseplate holes and the anchor shanks and between the anchor shanks and the surrounding concrete. Therefore, the attachment was idealized as an equivalent

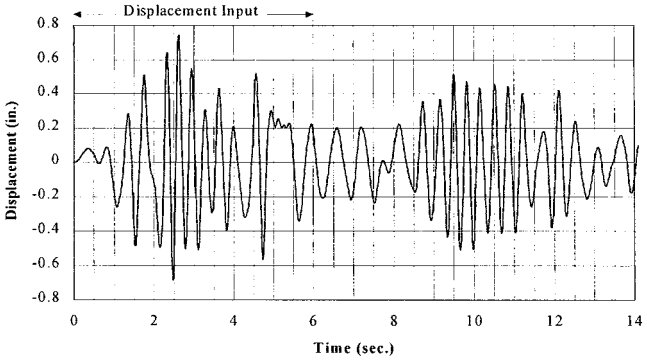

Fig. 10—History of estimated attachment displacement for seismic tests.

SDOF system (Fig. 8) with bilinear load-displacement behavior (Fig. 9). The initial lower-stiffness portion (40 kips/in., or 7000 kN/m), representing the effect of gaps on the baseplate, was estimated from the trial test. The higher-stiffness portion was taken as the initial stiffness of Fig. 7.

Using the idealized bilinear load-displacement behavior of Fig. 9 and the estimated mass of the attachment, the relative displacement response of the attachment at 12 in. (305 mm) was calculated numerically using the linear-acceleration method with the earthquake history of El Centro 1940 (NS component). That calculated displacement history is shown in Fig. 10. The most significant portion, consisting of the first 6.0 s of that record, was used as the command signal for the simulated earthquake loading. Each specimen was loaded repeatedly by that displacement input. As each test progressed, the input was scaled by larger and larger factors until failure occurred.

Basic mechanism for introducing concrete cracking

Some specimens had cracks with an initial width of 0.012 in. (0.3 mm). Wedge-type splitting tubes made of high-strength steel were used to crack the concrete specimens and widen the crack to the desired width. Each set consisted of a wedge and a pair of bearing split tubes (Fig. 11). Tapping the splitting wedge produced a large expansion force in the surrounding concrete.

Test procedure

During installation, anchors were torqued specified to the manufacturer's specifications. To simulate the reduction of prestressing force in anchors in service due to concrete relaxation, anchors were first fully torqued, then released after about 5 min to permit relaxation, and finally torqued again, but only to 50% of the specified torque.

For multiple-anchor shear tests, two separate cracks were initiated parallel to the loading direction. Because the baseplate was already fabricated, it was desired to control crack initiation so that as many anchors as possible could be installed directly in cracks. The following steps were used:

1. Drill four holes in the positions where the undercut anchors were to be installed, using a smaller drill bit than that required for the installation of anchors;
2. Place splitting tubes into PVC pipes and the drilled holes. Then tap the wedges one by one until a crack is visible. Remove splitting tubes;
3. Initiate another crack;
4. Drill the four holes again with a regular drill bit, then undercut them. Install anchors and the baseplate. Torque anchors, release, and retorque after about 5 min;
5. Place crack-measuring equipment on the cracks;

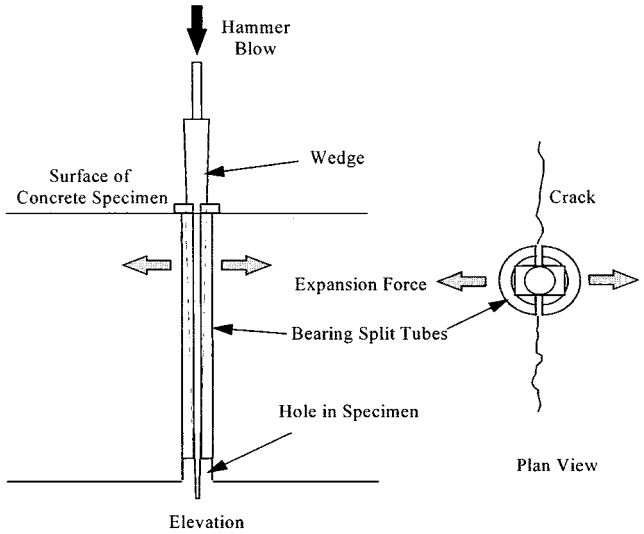

Fig. 11—Splitting tube for concrete cracking.

6. Place splitting tubes into PVC pipes. Tap wedges one by one to open the cracks to 0.3 mm; and

7. Set up the loading and data acquisition equipment. The crack widths were monitored during tests, but not controlled.

For static tests, the load was applied by slowly and monotonically adjusting the servo-controller to control the displacement of the hydraulic actuator, while monitoring the reading of the load cell to avoid any sudden increase of load.

For dynamic tests, the loading pattern was dynamic reversed cyclic loading (Fig. 10), applied under displacement control. During tests, the loading sequence was first applied with a maximum displacement of 0.6 in. (15.2 mm). If the connection did not fail, loading sequences were applied with maximum displacements of 1.0 in. (25 mm) and then 1.5 in. (38 mm). Further cycles, to a maximum displacement of 15 in. (38 mm), were applied until failure. Before each loading sequence, the anchors were hand-tightened to eliminate any initial lack of fit which would have increased the displacement required to reach any particular load level.

TEST RESULTS

Nomenclature

The test nomenclature consists of four-digit numbers (Zhang 1997). The first two digits specify the series of the test, while the last two digits specify the test number within Task 4. A complete listing of tests is given in Table 4. For example, Test 4206 represents a test in Series 4-2 and the sixth test of Task 4. For all tests, the edge distance was 5 in. (127 mm), and the embedment was 7 in. (178 mm).

Effect of dynamic reversed cyclic loading on behavior of multiple-anchor connections (UC1)

In Fig. 12 and 13, the load-displacement envelopes of dynamic tests under eccentric shear at 12 in. (305 mm) and 18 in. (457 mm), respectively, are compared with the static tests on the same configuration (Test 4101 versus Test 4203, and Test 4102 versus Test 4206). The following observations can be made:

1. The dynamic load-displacement curves follow the static load-displacement curves over most of the displacement range, differing only near the ultimate load;

2. The maximum dynamic capacity was close to the maximum static capacity. It was 7% higher at a 12 in. (305 mm) eccentricity, and 7% smaller at an 18 in. (457 mm) eccentricity.

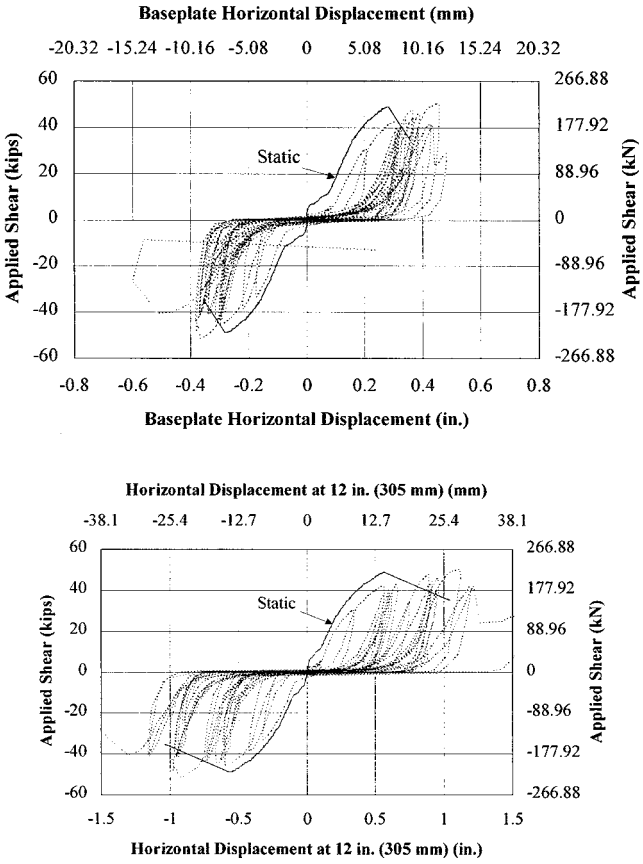

Fig. 12—Comparison of static and seismic load-displacement behaviors of multiple-anchor connections with UC1 anchors under shear at 12 in. (305 mm) eccentricity (Tests 4101 and 4203, respectively).

Due to the small number of tests, however, this observation is not definitive; and

3. The most significant effect of dynamic reversed cyclic loading is the increase in total displacement, measured at 12 in. (305 mm) above the concrete specimen. As shown in Fig. 12 and 13, the displacement at the baseplate increased by about 0.1 in. (2.54 mm) at a 12 in. (305 mm) eccentricity, but not at all at an 18 in. (457 mm) eccentricity (probably due to the smaller load). The increase in horizontal displacement of the baseplate was due mainly to spalling of the concrete in front of the anchors. It was also due to the gaps between the baseplate and the anchors as well as between the anchors and the concrete. The increase in the displacement measured at 12 in. (305 mm) above the concrete specimen was much greater, mainly because of the larger tensile displacement of the anchors under dynamic cyclic loading.

Test 4307 (on a connection with EAII under dynamic reversed cyclic loading) also showed large displacements of about 1 in. (25.4 mm) measured at 12 in. (305 mm) above the concrete, although there is no corresponding static test with which this can be compared.

Effect of baseplate flexibility on load-displacement behavior of multiple-anchor connection

Test 4203 and 4205 were identical except for baseplate flexibility. Test 4203 had a flexible baseplate while Test 4205 had a rigid one; both had UC1 anchors, and were loaded in dynamic eccentric shear at an eccentricity of 12 in. (305 mm). Their load-displacement behavior is compared as follows:

Table 4—Test matrix for eccentric shear tests on multiple-anchor connections

Test	Description	Concrete	Anchor
4101	Static, four-anchor group, rigid baseplate, uncracked concrete, e = 12 in. (305 mm)	4700 lb/in.^{2} (32.4 MPa)	UC1 5/8 in. (16 mm)
4102	Static, four-anchor group, rigid baseplate, uncracked concrete, e = 18 in. (457 mm)	4700 lb/in.^{2} (32.4 MPa)	UC1 5/8 in. (16 mm)
4203	Dynamic, four-anchor group, flexible baseplate, uncracked concrete, e = 12 in. (305 mm)	4700 lb/in.^{2} (32.4 MPa)	UC1 5/8 in. (16 mm)
4204	Dynamic, four-anchor group, rigid baseplate, uncracked concrete, e = 12 in. (305 mm)	4700 lb/in.^{2} (32.4 MPa)	UC1 5/8 in. (16 mm)
4205	Dynamic, four-anchor group, rigid baseplate, uncracked concrete, e = 12 in. (305 mm)	4700 lb/in.^{2} (32.4 MPa)	UC1 5/8 in. (16 mm)
4206	Dynamic, four-anchor group, rigid baseplate, uncracked concrete, e = 18 in. (457 mm)	4700 lb/in.^{2} (32.4 MPa)	UC1 5/8 in. (16 mm)
4307	Dynamic, four-anchor group, rigid baseplate, cracked concrete, e = 12 in. (305 mm)	4700 lb/in.^{2} (32.4 MPa)	EAII 5/8 in. (16 mm)
4308	Dynamic, four-anchor group, rigid baseplate, cracked concrete, e = 12 in. (305 mm)	4700 lb/in.^{2} (32.4 MPa)	UC1 5/8 in. (16 mm)
4309	Dynamic, four-anchor group, rigid baseplate, cracked concrete, e = 18 in. (457 mm)	4700 lb/in.^{2} (32.4 MPa)	UC1 5/8 in. (16 mm)
4310	Dynamic, four-anchor group, rigid baseplate, cracked concrete, e = 18 in. (457 mm)	4700 lb/in.^{2} (32.4 MPa)	EAII 5/8 in. (16 mm)
4411	Static, near-edge, four-anchor group, rigid baseplate, uncracked concrete, no hairpins, e = 12 in. (305 mm)	4700 lb/in.^{2} (32.4 MPa)	UC1 5/8 in. (16 mm)
4412	Static, near-edge, four-anchor group, rigid baseplate, uncracked concrete, no hairpins, e = 18 in. (457 mm)	4700 lb/in.^{2} (32.4 MPa)	UC1 5/8 in. (16 mm)
4513	Dynamic, near-edge, four-anchor group, rigid baseplate, uncracked concrete, no hairpins, e = 12 in. (305 mm)	4700 lb/in.^{2} (32.4 MPa)	UC1 5/8 in. (16 mm)
4514	Dynamic, near-edge, four-anchor group, rigid baseplate, uncracked concrete, no hairpins, e = 18 in. (457 mm)	4700 lb/in.^{2} (32.4 MPa)	UC1 5/8 in. (16 mm)
4615	Static, near-edge, four-anchor group, rigid baseplate, uncracked concrete, close hairpins, e = 12 in. (305 mm)	4700 lb/in.^{2} (32.4 MPa)	UC1 5/8 in. (16 mm)
4616	Dynamic, near-edge, four-anchor group, rigid baseplate, uncracked concrete, close hairpins, e = 12 in. (305 mm)	4700 lb/in.^{2} (32.4 MPa)	UC1 5/8 in. (16 mm)
4617	Dynamic, near-edge, four-anchor group, rigid baseplate, uncracked concrete, close hairpins, e = 18 in. (457 mm)	4700 lb/in.^{2} (32.4 MPa)	UC1 5/8 in. (16 mm)

1. Baseplate flexibility led to no significant change in capacity. The capacity in Test 4203 was only about 2.7% smaller than in Test 4205. Since the plastic deformation was very small, there should be little effect on the distribution of tension forces to the anchors; and

2. The displacement measured 12 in. (305 mm) above the base was a little larger in Test 4203 (flexible baseplate) than in Test 4205 (rigid baseplate), while the displacement measured at the baseplate itself was a little smaller for Test 4203. This may be attributed to the slight deformation of the baseplate observed in test, which increase the amount of rotation of the attached member, and also the measured displacement at 12 in. above the concrete.

The significance of these results must be interpreted carefully, however, because both baseplates had stiffeners. If the more flexible baseplate had not been provided with stiffeners, its behavior would have been quite different.

Comparison of dynamic tests of multiple-anchor connections in cracked concrete with static tests in uncracked concrete

In Fig. 14 and 15, the load-displacement curves for tests with dynamic loading in cracked concrete (Test 4308 and 4309) are compared with the corresponding for tests with static loading in tests in uncracked concrete (Test 4101 and 4102).

The dynamic load-displacement envelopes for these tests also follow the static load-displacement curves well, except near the ultimate load. This tendency was also noted for dynamic tests in uncracked concrete.

Effect of cracks on load-displacement behavior of multiple-anchor connections under dynamic reversed loading

To compare the dynamic load-displacement behavior of multiple-anchor connections in cracked and uncracked concrete, their load-displacement curves are compared as above, and two characteristic values are also compared: the maximum load reached during the test; and the maximum displacement reached in the test before the connection failed, measured 12 in. (305 mm) above concrete surface. These are compared in Fig. 16 and 17. From left to right in those figures, the results correspond to Test 4204, 4307, 4205, 4308, 4206, and 4309.

For UC1, the maximum load reached in dynamic tests in uncracked concrete (Series 4-2) was about the same as in uncracked concrete (Fig. 16). The displacement at failure, however, increased for dynamic tests at both eccentricities in cracked concrete as compared with uncracked (Fig. 17). This is because the cracking allowed the anchor heads to slip and expand further with the extra space created by the additional crack opening.

For EAII, dynamic tests at a loading eccentricity of 12 in. (305 mm) reached greater displacement in cracked than in uncracked concrete; the capacity decreased by 13%, although both connections failed by tensile fracture of anchor steel. Due to the small number of tests, conclusions regarding capacity are tentative.

In the dynamic test on the connection with EAII at 12 in. (305 mm) eccentricity, the horizontal displacement of the baseplate was much larger than in the corresponding test in uncracked concrete, even though the external load was smaller. This observation correlated with the extensive concrete spalling observed at the front anchors at both directions. This spalling is attributed to the large number of cycles of loading, and to the low shearing stiffness of the anchors.

The dynamic test on a connection with EAII in cracked concrete at an 18 in. (457 mm) eccentricity resulted in gross pull-out failure of the anchors, all of which pulled out about

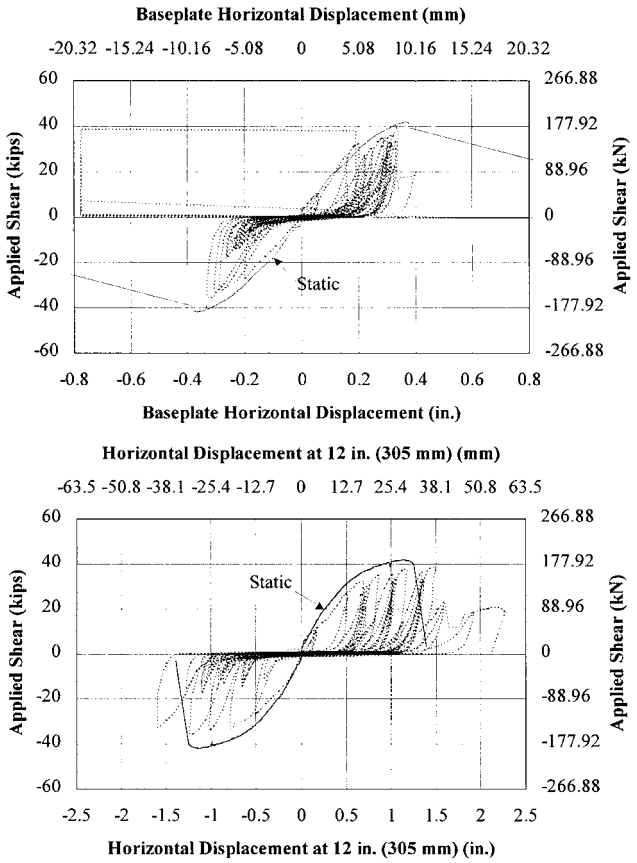

Fig. 13—Comparison of static and seismic load-displacement behaviors of multiple-anchor connections with UC1 anchors under shear at 18 in. (457 mm) eccentricity (Test 4102 and 4206, respectively).

3 in. (76 mm). This confirms the observation in the single-anchor tests of Rodriguez (1995) that EAII could lose capacity due to a change of failure mode (from cone breakout to pull-out) under dynamic loading. This undesirable characteristic is exacerbated in cracked concrete.

Effect of concrete edges on multiple-anchor connections under static loading

Near-edge, multiple-anchor connections without hairpins, loaded statically in eccentric shear, exhibited two-peaked load-displacement behavior similar to that of double-anchor shear connections without hairpins (Hallowell 1996). The first peak occurred when the concrete edge broke out under shear of the front anchors; the second peak occurred at a much larger displacement, when the back anchors fractured.

Figure 18 shows the loads corresponding to edge breakout and steel failure, without hairpins (Test 4411) and with close hairpins (Test 4615), with a 12 in. (305 mm) loading eccentricity. The edge breakout load was almost identical at the larger eccentricity of 18 in. (457 mm).

Using the BDA5 program (discussed later in this paper), the calculated capacity corresponding to fracture of the back anchors was 32.9 kips (146 kN) for the connection with a 12 in. (305 mm) loading eccentricity, and 27.6 kips (123 kN) for the connection with an 18 in. (457 mm) loading eccentricity. These are 8.1% and 9.3% lower, respectively, than the test results. From the curves of tensile forces in the anchors versus the applied loading

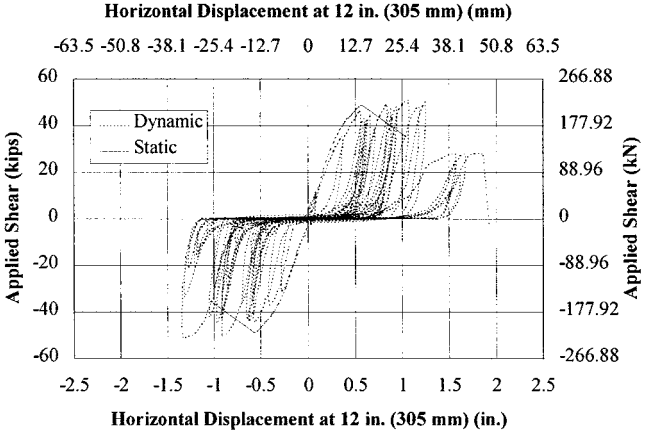

Fig. 14—Comparison of seismic load-displacement behavior of multiple-anchor connections with UC1 anchors at 12 in. (305 mm) eccentricity in cracked concrete (Test 4308) with static behavior in uncracked concrete (Test 4101).

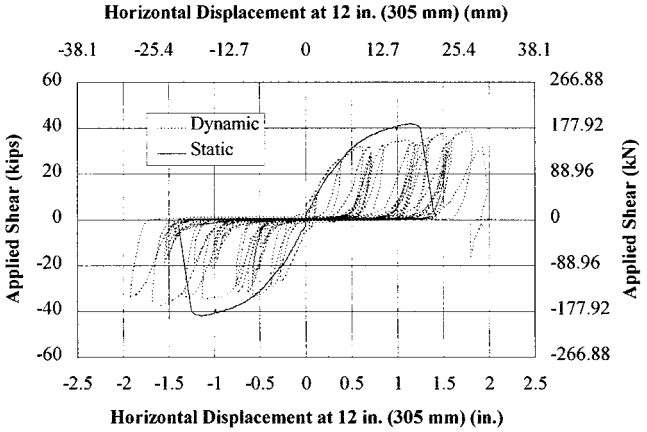

Fig. 15—Comparison of seismic load-displacement behavior of multiple-anchor connections with UC1 anchors at 18 in. (457 mm) eccentricity in cracked concrete (Test 4309) with static behavior in uncracked concrete (Test 4102).

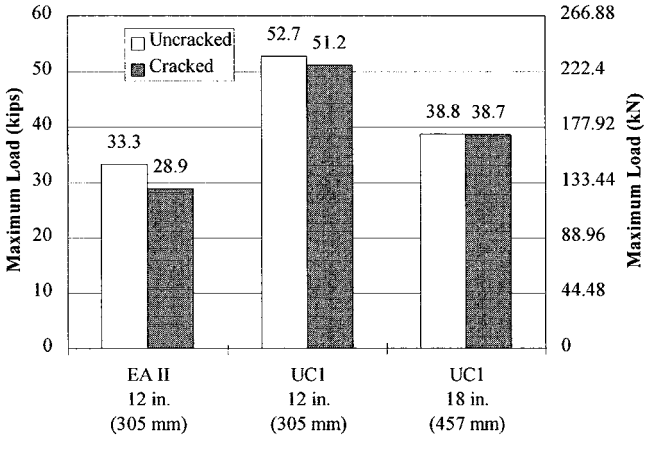

Fig. 16—Effect of cracks on dynamic response of multiple-anchor connections.

(Zhang 1997, Appendix D), it is apparent that at both loading eccentricities some tension remained in the two front anchors when the back anchors fractured. It is reasonable to conclude that some shear force still remained in the front anchors as well, resulting in higher tested capacities.

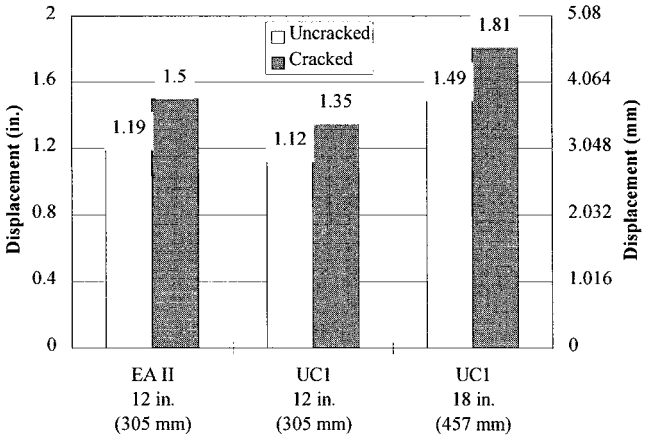

Fig. 17—Maximum displacement at 12 in. (305 mm) above concrete surface of multiple-anchor connections under dynamic reversed loading in cracked and uncracked concrete.

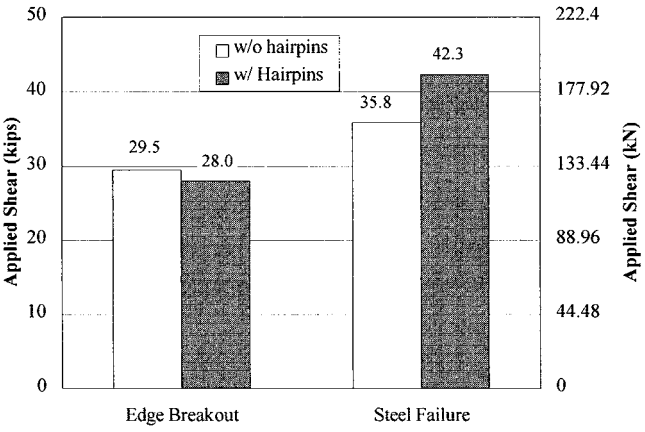

Fig. 18—Capacity of near-edge, multiple-anchor connections with UC1 anchors under static loading with and without hairpins, 12 in. (305 mm) loading eccentricity.

Effect of concrete edges on multiple-anchor connections under dynamic reversed loading

In Fig. 19, the concrete edge breakout capacities of multiple-anchor connections without hairpins are compared for dynamic and static loading. Edge breakout capacity under dynamic load is virtually the same as under static load. This contrasts with increase in edge breakout capacity observed under dynamic loading for double-anchor shear connections (Zhang 1997, Section 5.16). The explanation is believed to lie in the difference in loading program for the two types of tests. The double-anchor shear tests were conducted using ramp loading to failure. The multiple-anchor connection tests were also conducted at dynamic loading rates, but using the complex history of Fig. 10. Concrete breakout occurred near the maximum command displacement, when the imposed velocity (rate of loading) was much smaller than in the ramp loading tests.

After concrete edge breakout under loading in one direction, capacity in the other direction dropped very quickly, due to lateral pryout of the near-edge anchor heads that had previously experienced edge breakout. In specimens without hairpins, the concrete breakout volume was very large, the concrete cover to the near-edge anchor heads was lost, and the lateral pryout capacity of the near-edge anchors dropped significantly.

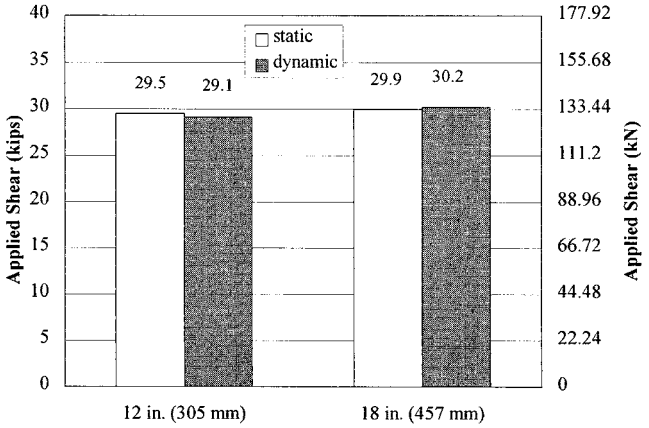

Fig. 19—Concrete breakout loads of near-edge, multiple-anchor connections with UC1 anchors without hairpins under static and dynamic loading.

Effect of close hairpins on behavior of multiple-anchor connection under static loading

Figure 18 compares the concrete breakout capacity and the maximum capacity of multiple-anchor connections, without hairpins and with close hairpins, under static loading at a 12 in. (305 mm) eccentricity. As noted by Malik, Mendonca, and Klingner (1982), hairpins have little effect on edge breakout load, because breakout must occur before the hairpin is effective. Hairpins, however, greatly enhance post-breakout strength and ductility. In near-edge, multiple-anchor connections with close hairpins, the near-edge anchors retain more shear after concrete breakout than otherwise identical anchors without hairpins. In these tests, connections with close hairpins had 18% higher capacity, and a much more gradual drop in capacity after edge breakout.

Effect of dynamic reversed loading on near-edge multiple-anchor connections with hairpins

Figure 20 compares the static and dynamic load-displacement behaviors (Test 4615 and 4616, respectively) of near-edge, multiple-anchor connections with hairpins, loaded at a 12 in. (305 mm) eccentricity. As before, the envelope of the dynamic response basically follows the static response.

In Fig. 21, the concrete breakout capacity and the maximum capacity toward the free edge are shown, for static and reversed dynamic loading (Test 4615 and 4616). As before, concrete breakout capacity is almost the same under dynamic and static loading. Maximum dynamic capacity, however, is about 9% higher than static. As shown in Fig. 20, the postpeak dynamic envelope is close to the static response.

Effect of close hairpins on load-displacement behavior of near-edge, multiple-anchor connections under dynamic reversed loading

Figure 22 compares the concrete edge breakout capacity and the maximum capacity achieved in both directions, without hairpins (Test 4513) and with close hairpins (Test 4616), for near-edge multiple-anchor connections loaded at a 12 in. (305 mm) eccentricity. Figure 23 shows the same comparison for connections with an 18 in. (457 mm) eccentricity (Test 4514 and 4617, respectively).

For the connections with 12 in. (305 mm) eccentricity, close hairpins had little effect on concrete breakout capacity, but significantly increased maximum capacity. The maximum load achieved toward the specimen edge was 55% higher with hairpins, than without.

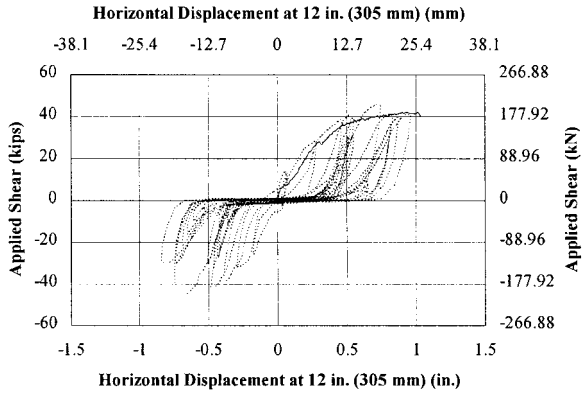

Fig. 20—Comparison of load-displacement behavior of near-edge, multiple-anchor connections with UC1 anchors with hairpins, under static and seismic loading.

Hairpins had little effect on the load-displacement behavior of the near-edge, multiple-anchor connections loaded at an 18 in. (457 mm) eccentricity. This is because the capacity of that connection was controlled by the anchors' tensile capacity rather than their shear capacity.

Comparison of test results for multiple-anchor connections at large edge distances with predictions of BDA5 program

Introduction to BDA5 program—The BDA5 program is a macromodel program developed at the University of Stuttgart for the static analysis of multiple-anchor connections loaded by eccentric shear (Li 1994). It requires as input data a complete set of load-displacement curves of the anchor under oblique loading at angles from 0 to 90 degrees. In the program, the baseplate is assumed rigid, and the compressive stress distribution on the concrete under the baseplate is simplified as linear, with a maximum compressive stress not exceeding f_c'. Each row of anchors is modeled as a nonlinear spring, whose load-displacement properties are obtained by interpolating between the input load-displacement curves for the anchor. Appendix E of Zhang (1997) gives an example input file for the BDA5 program. The calculated results from the program are given in terms of horizontal displacement and rotation of the baseplate, and vertical displacement at the center of the baseplate.

In Task 2 of this research project, the BDA5 program was extensively examined with test results from two-anchor connections, using load-displacement curves obtained from single-anchor tests. Its accuracy and validity were demonstrated for a wide range of loading eccentricities (Lotze and Klingner 1997). However, it sometimes has difficulties in convergence.

Calculation of load and displacement behaviors of multiple-anchor connections using BDA5 program—Many multiple-anchor connection tests of this study used UC1 of 5/8 in. (16 mm) diameter. Figure 24 shows a complete set of load-displacement curves for that anchor, obtained by Lotze and Klingner (1997) in Task 2 of this research program. Those curves are used here as input data for the BDA5 program.

In Fig. 25 and 26, observed load-displacement results for the multiple-anchor connections of this study, with UC1 anchors, loaded at eccentricities of 12 in. (305 mm) and 18 in. (457 mm), respectively (Test 4101 and 4102), are compared with predictions from the BDA5 program. The starting points of some curves were shifted horizontally in the plots, explained as follows.

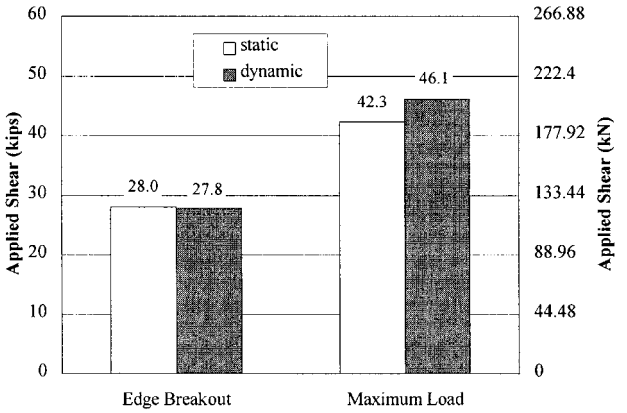

Fig. 21—Comparison of capacities of near-edge, multiple-anchor connections with UC1 anchors with hairpins, under static and dynamic loading toward specimen edge.

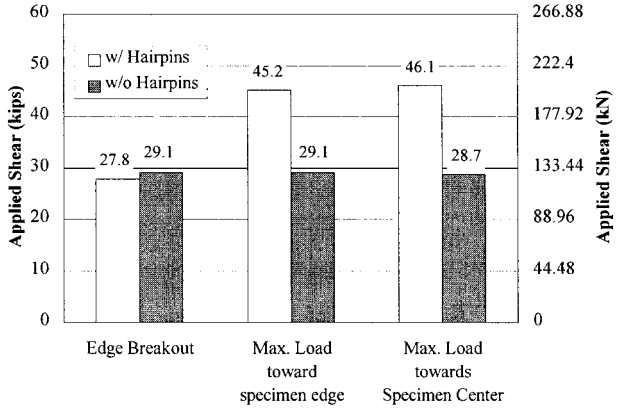

Fig. 22—Dynamic capacities of near-edge, multiple-anchor connections with UC1 anchors, with and without hairpins, loaded at 12 in. (305 mm) eccentricity.

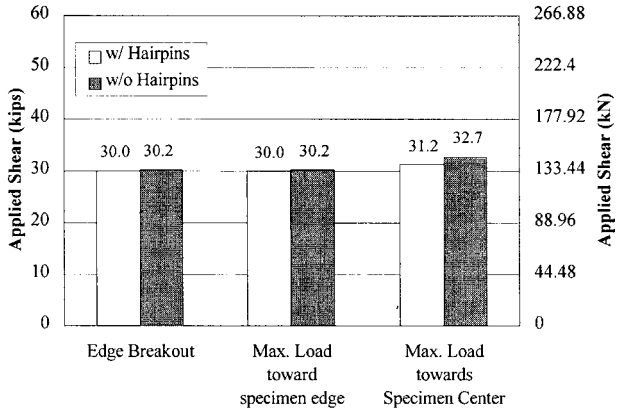

Fig. 23—Dynamic capacities of near-edge, multiple-anchor connections with and without hairpins, loaded at 18 in. (457 mm) eccentricity.

As seen from Fig. 25 and 26, the predicted load-displacement curves are initially much stiffer than the observed ones. At higher loads, however, the predicted behavior matches that of the observed, especially for the displacement at 12 in. (305 mm) above the concrete surface. The lower observed stiffness at lower loads could be attributed to the uneven concrete surface, the uneven baseplate, or the gaps between the anchor shanks and the baseplate and the anchor shanks and surrounding concrete. If the rigid-body motion of the attachment had been due only to slip, the difference between

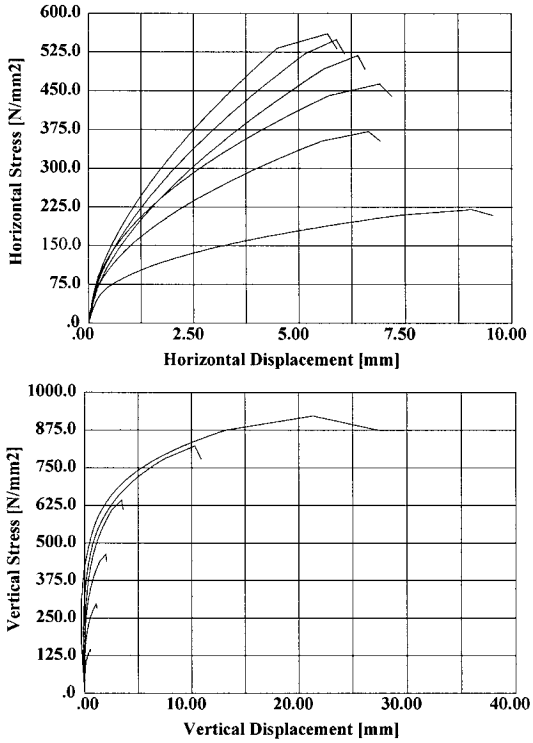

Fig. 24—Typical load-displacement curves for single UC1 anchor loaded at various angles (Lotze and Klingner 1997).

calculated and observed horizontal displacement would have been the same anywhere on the attachment. The fact that the difference between predicted and observed displacement was greater at 12 in. (305 mm) above the concrete surface than at the surface indicates rigid-body rotation of the attachment, due either to imperfections on the concrete surface or welding-induced distortion of the baseplate. In the input load-displacement curves of BDA5 program, the effect of gaps was completely ignored, and the concrete surface and the baseplate were assumed level. These factors might be modeled with the BDA5 program by reducing the stiffness of the input load-displacement curves in the low-load range.

Using the BDA5 program, the maximum capacity of the connection with an 18 in. (457 mm) loading eccentricity was predicted accurately. The maximum capacity of the connection with a 12 in. (305 mm) eccentricity, however, was less than predicted, even though the predicted failure mode, shear fracture of the front anchor, was in fact observed during the test. The overprediction could have been due to premature failure of one of the shear anchors due to unevenly distributed shear force, since only one compression anchor failed during the test.

In Fig. 27 and 28, the predicted behavior, shifted to the right to match the test results at higher loads, is again compared with the static and dynamic test results. The predicted behavior agrees well with that observed for the static tests, and with the envelope of the dynamic tests.

Comparison of test results with plastic method and modified plastic method of multiple-anchor connections at large edge distances

The Plastic Method (Cook and Klingner 1992) and the Modified Plastic Method (Lotze and Klingner 1997) predict the capacity of multiple-anchor connections with large edge distances, loaded in shear and failing by steel fracture. In this section, test results from this study for

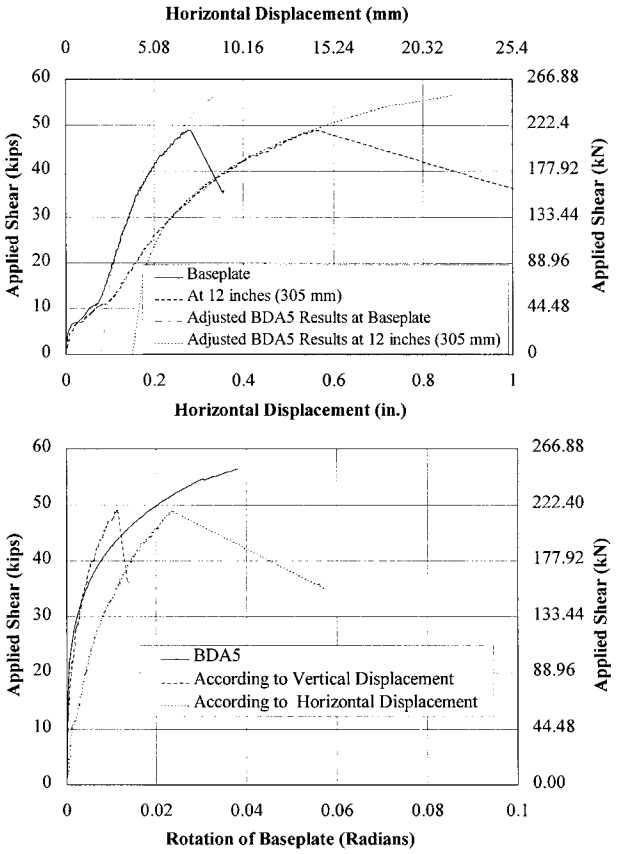

Fig. 25—Comparison of calculated results from BDA5 program with static test results for multiple-anchor connection with UC1 anchors at 12 in. (305 mm) eccentricity (Test 4101).

multiple-anchor connections with UC1 anchors, loaded in shear, are compared with the predictions of both methods and of the BDA5 program.

For the tested connections using a friction coefficient of 0.15, the critical eccentricity e_2 at which the tension anchors begin to resist some of the applied shear (Cook and Klingner 1992), is

$$e_2 = 12 \text{ in.}/(0.15 + 0.6) = 16 \text{ in. (406 mm)}$$

The loading eccentricities used in these tests, 12 and 18 in. (305 and 457 mm), were selected because they lie on either side of that critical eccentricity. The calculated capacities of connections with 5/8 in. (16 mm) UC1 are compared in Fig. 29 with the test results, based on the average of tested anchor capacity (Cook 1989) of 31.0 kips (138 kN) in tension, and 18.6 kips (82.7 kN) in shear.

For the connection with a loading eccentricity of 18 in. (457 mm), the capacities calculated by the Plastic Method and the BDA5 program are very close to the test results. The Modified Plastic Method (Lotze and Klingner 1997), however, underestimated the static capacity by as much as 10%.

For the connection with a loading eccentricity of 12 in. (305 mm), both the Plastic Method and the BDA5 program overestimated the static capacity. The Modified Plastic Method (Lotze and Klingner 1997) was very close to the test results. As mentioned before, however, the connection with a 12 in. (305 mm) eccentricity might have failed prematurely in the static test, because of unevenly distributed shear force to the shear anchors.

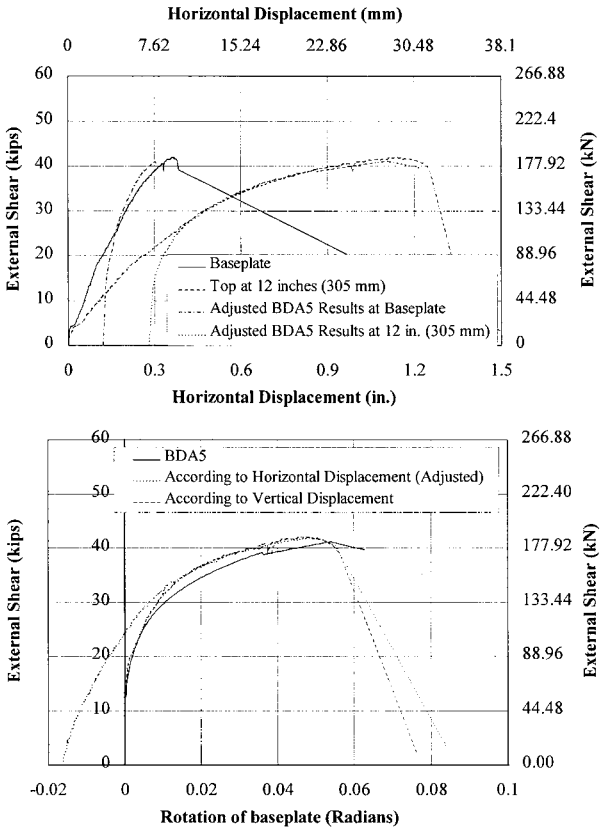

Fig. 26—Predictions of BDA5 program versus static test results for multiple-anchor connection with UC1 anchors at 18 in. (457 mm) eccentricity (Test 4102).

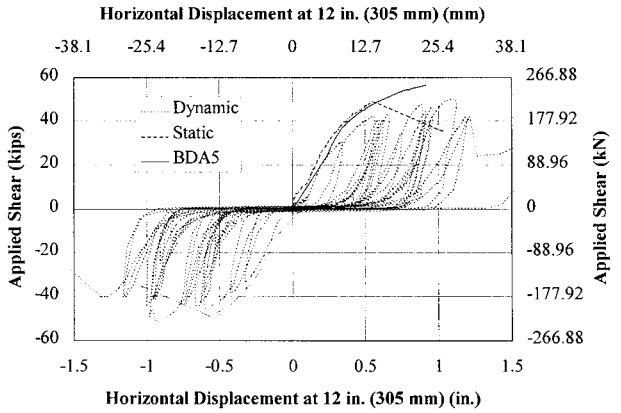

Fig. 27—Predictions of BDA5 program versus static and seismic test results of multiple-anchor connection with UC1 anchors loaded in eccentric shear at 12 in. (305 mm).

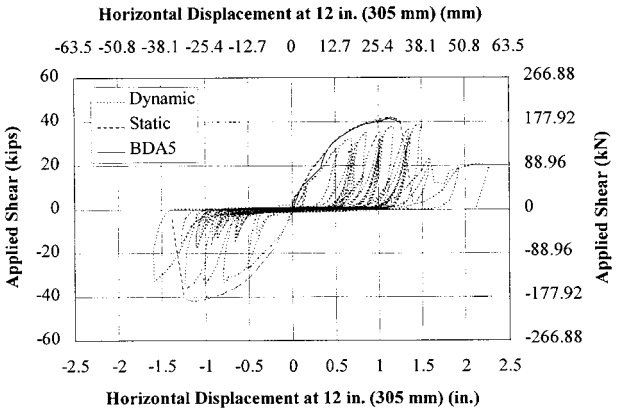

Fig. 28—Predictions of BDA5 program versus static and seismic test results of multiple-anchor connection with UC1 anchors loaded in eccentric shear at 18 in. (457 mm).

SUMMARY, CONCLUSIONS, AND RECOMMENDATIONS

Summary

This research project, supported by the U.S. Nuclear Regulatory Commission at the University of Texas at Austin, was intended to assess the seismic behavior of single- and multiple-anchor connections in cracked and uncracked concrete. It included study of single anchors under tensile loading; single anchors under oblique tensile loading; double-anchor connections under tensile loading; single near-edge anchors under shear loading; near-edge double-anchor connections under eccentric shear loading; and multiple-anchor connections under shear at small eccentricities.

This paper deals with the seismic behavior of multiple-anchor connections to concrete. It summarizes information previously presented in Zhang (1997). The purpose of the multiple-anchor connection tests was to assess the effect of earthquake-type loading on the behavior of connections under various conditions, including anchor types, hairpins, concrete cracking, and proximity to member edges. The seismic load-displacement response of a multiple-anchor connection was estimated and subsequently used as a dynamic loading input to the connection.

Anchors were installed with full embedment. Two eccentricities of shear load were used in tests, with the emphasis on the smaller eccentricity, at which the tension anchors would be subjected to both tension and shear. Multiple-anchor connections were loaded dynamically under a simulated earthquake-type, reversed cyclic loading. Static tests were also conducted for comparison.

Conclusions

Conclusions from multiple-anchor connection tests—

1. Multiple-anchor connections in uncracked or cracked concrete, with or without edge effects, and with or without hairpins, loaded dynamically under reversed cyclic loading histories representative of seismic response, behaved consistently with the results of previous single- and double-anchor tests of this study. Previous observations regarding the load-displacement behavior, and failure mechanisms of single and double anchors, were applicable in predicting the behavior of complex, multiple-anchor connections under simulated seismic loading. The implications of this are clear. Multiple-anchor connections designed for ductile behavior in uncracked concrete under static loading, will probably still behave in a ductile manner in cracked concrete under dynamic loading;

2. Anchors that show relatively good performance when tested individually in cracked concrete (CIP headed anchors, UC1, and 20 mm diameter Sleeve) will probably also show relatively good performance in multiple-anchor connections subjected to seismic loading. Anchors that show relatively poor performance when tested individually in cracked concrete (Grouted Anchor, EAII, and 10 mm diameter Sleeve) will probably also show relatively poor performance in multiple-anchor connections subjected to seismic loading;

3. Cyclic load-displacement behavior of multiple-anchor connections is accurately bounded by the corresponding static load-displacement envelope, and also by the static load-

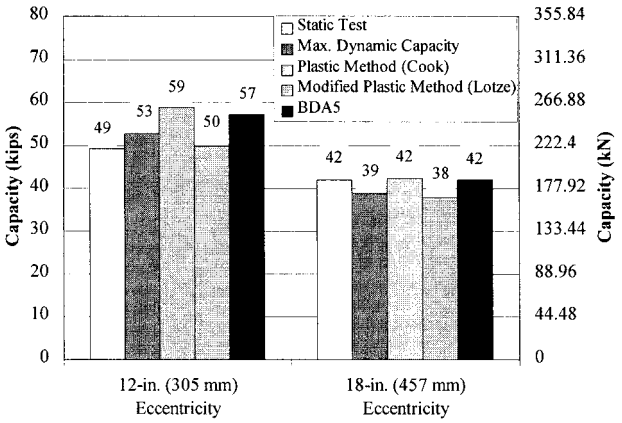

Fig. 29—Tested versus calculated capacities of multiple-anchor connections with UC1 anchors, at large edge distances, loaded in shear.

displacement envelope predicted by the BDA5 program. Dynamic cycling does not significantly influence the fundamental load-displacement behavior of multiple-anchor connections;

4. Under dynamic reversed cyclic loading in both uncracked and cracked concrete, the load-displacement envelopes of multiple-anchor connections with the UC1 anchor basically follow the static curves in uncracked concrete over most displacements, differing only near the ultimate load. Dynamic reversed loading did not significantly affect the maximum dynamic capacity. In uncracked concrete, the connection had larger displacements under reversed dynamic than under static loading. Under dynamic reversed loading, connections in cracked concrete had slightly larger displacements than those in uncracked concrete;

5. Under dynamic reversed cyclic loading, multiple-anchor connections with EAII had very large displacements. In both uncracked and cracked concrete, the connections loaded at 12 in. (305 mm) eccentricity failed by steel fracture. The test in cracked concrete had a larger displacement and smaller capacity than that in uncracked concrete. The connection loaded at an 18 in. (457 mm) eccentricity experienced gross pull-out failure of the anchors;

6. Thickness of stiffened baseplates had little effect on the dynamic load-displacement behavior of multiple-anchor connections, even though the moment applied to the baseplate at the edge of the attached member (by the compression reaction of the concrete) exceeded the tested yield moment of the baseplate by about 25%. Baseplate thickness would probably have been significant had the baseplates not been stiffened;

7. The concrete edge breakout capacity remained almost constant for near-edge, multiple-anchor connections of UC1 anchors with both eccentricities, under static loading with or without hairpins, and under dynamic reversed cyclic loading with hairpins;

8. Hairpins increased the ultimate capacity toward the edge, of near-edge, multiple-anchor connections. This capacity can be accurately predicted by assuming a flexural mechanism in the near-edge anchors (Malik, Mendonca, and Klingner 1982). Hairpins also reduced the concrete edge breakout volume and increased the lateral blowout capacity of near-edge anchors, thereby increasing the maximum capacity for loading away from the edge of those same connections;

9. Local forces induced by the baseplate on the edge breakout volume of near-edge, multiple-anchor connections significantly reduced the concrete edge breakout capacity; and

10. The capacity of multiple-anchor connections at large edge distances was predicted with reasonable accuracy by the original Plastic Method of Cook and Klingner (1992), the Modified Plastic Method of Lotze and Klingner (1997), and the Modified Plastic Method of Zhang (1997). Because insufficient test data are available for a comprehensive comparison, this evaluation is based partly on predicted capacities from the BDA5 program.

Conclusions regarding BDA5 program—The BDA5 program (Li 1994) generally gives reasonable, quick predictions of the load-displacement behavior of multiple-anchor connections. It relies heavily, however, on input data describing the load-displacement behavior of single anchors. Since load-displacement behavior varies with anchor type, diameter and embedment, many tests are required to obtain these input data.

ACKNOWLEDGMENTS

This paper presents partial results of a research program supported by the U.S. Nuclear Regulatory Commission (NRC) (NUREG/CR-5434, "Anchor Bolt Behavior and Strength during Earthquakes"). The technical contact is Herman L. Graves, III, whose support is gratefully acknowledged. The conclusions in this paper are those of the authors only, and are not NRC policy or recommendations.

REFERENCES

ACI Committee 349, 1990, "Code Requirements for Nuclear Safety Related Concrete Structures, (ACI 349-90)," American Concrete Institute, Farmington Hills, Mich., 123 pp.

Cannon, R. W., 1981, "Expansion Anchor Performance in Cracked Concrete," ACI JOURNAL, *Proceedings* V. 78, No. 6, Nov.-Dec., pp. 471-479.

CEB, 1991, "Fastenings to Reinforced Concrete and Masonry Structures: State-of-Art Report, Part 1," Euro-International Concrete Committee (CEB), Aug.

Collins, D.; Klingner, R. E.; and Polyzois, D., 1989, "Load-Deflection Behavior of Cast-in-Place and Retrofit Concrete Anchors Subjected to Static, Fatigue, and Impact Tensile Loads," *Research Report CTR 1126-1*, Center for Transportation Research, University of Texas at Austin, Feb.

Cook, R. A., 1989, "Behavior and Design of Ductile Multiple-Anchor Steel-to-Concrete Connections," PhD dissertation, University of Texas at Austin, May.

Cook, R. A., and Klingner, R. E., 1992, "Ductile Multiple-Anchor Steel-to-Concrete Connections," *Journal of Structural Engineering*, ASCE, V. 118, No. 6, June, pp. 1645-1665.

Copley, J. D., and Burdette E. G., 1985, "Behavior of Steel-to-Concrete Anchorage in High Moment Regions," ACI JOURNAL, *Proceedings* V. 82, No. 2, Mar.-Apr., pp. 180-187.

Eibl, J., and Keintzel, E., 1989, "Zur Beanspruchung von Befestigungsmitteln bei dynamischen Lasten," *Forschungsbericht T2169*, Institut für Massivbau und Baustofftechnologie, Universität Karlsruhe.

Eligehausen, R., and Balogh, T., 1995, "Behavior of Fasteners Loaded in Tension in Cracked Reinforced Concrete," *ACI Structural Journal*, V. 92, No. 3, May-June, pp. 365-379.

Fuchs, W.; Eligehausen, R.; and Breen, J. E., 1995, "Concrete Capacity Design (CCD) Approach for Fastening to Concrete," *ACI Structural Journal*, V. 92, No. 1, Jan.-Feb., pp. 73-94.

Hallowell, J. M., 1996, "Tensile and Shear Behavior of Anchors in Uncracked and Cracked Concrete under Static and Dynamic Loading," MS thesis, University of Texas at Austin, Dec.

Klingner, R. E.; Hallowell, J. M.; Lotze, D.; Park, H.-G.; Rodriguez, M.; and Zhang, Y.-G., 1998, *Anchor Bolt Behavior and Strength during Earthquakes*, Report prepared for the U.S. Nuclear Regulatory Commission (NUREG / CR-5434), Aug.

Li, L., 1994, *Programm zur Berechnung des Trag- und Verformungsverhaltens von Gruppenbefestigungen unter kombinierter Schragzug- und Momentenbeanspruchung (Programmbeschreibung)*, University of Stuttgart, June.

Lotze, D., and Klingner, R. E., 1997, "Behavior of Multiple-Anchor Connections to Concrete From the Perspective of Plastic Theory," *PMFSEL Report* No. 96-4, University of Texas at Austin, Mar.

Malik, J. B.; Mendonca, J. A.; and Klingner, R. E., 1982, "Effect of Reinforcing Details on the Shear Resistance of Short Anchor Bolts under Reversed Cyclic Loading," ACI JOURNAL, *Proceedings* V. 79, No. 1, Jan.-Feb., pp. 3-11.

Rodriguez, M., 1995, "Behavior of Anchors in Uncracked Concrete under Static and Dynamic Loading," MS thesis, University of Texas at Austin, Aug.

Zhang, Y., 1997, "Dynamic Behavior of Multiple-Anchor Connections in Cracked Concrete," PhD dissertation, Department of Civil Engineering, University of Texas at Austin, Aug.